A novel approach for Human Action Recognition

Dr. Upasana Sinha
Associate Professor,
Department of CSE
J. K. Institute of Eng, CG, India

Dileshwar Patel
Assistant Professor,
Department of CSE
J. K. Institute of Eng, CG, India

Jyoti Yadav
Associate Professor,
Department of CSE
J. K. Institute of Eng, CG, India

Abstract: We propose a new neighborhood descriptor based on Finite Element Analysis for human development. That's the closest thing to a descriptor when it comes to human postures. If you're interested in learning more about this framework, please contact us at or . As soon as the schematic structure begins, it addresses the human constitution. The diagram's most unusual components are then selected. In order to detect the cutoff points, the vertices of the triangles are used. Each triangle's strength system is then determined. On the development video body trademark vector, all strength systems of each and every functional triangle are joined together as a reference. The RBF-SVM classifier uses these trademark vectors. Weizmann, KTH, Ballet and IXMAS datasets indicate that the suggested strategy outperforms other current methods.

Keywords: finite element analysis (FEA), stiffness matrix, discretization, support vector machine

I. INTRODUCTION

In the last two decades, PCs have revolutionized human existence in almost every way imaginable. It's no longer a secret that video content has become increasingly accessible and popular in recent years. Cell phones, tablets, and high-tech cameras have become more powerful as technology advances. Additionally, the growing number of available recordings has increased the desire to obtain them. For this reason, a large number of recordings have been analyzed to determine the activity. Clinical, sports, and security fields all benefit from activity recognition.

During the last few decades, it's been discovered that PC frameworks have had a profound impact on human life in practically every conceivable way. Video reality has become more and more accessible and prevalent in the contemporary day because of the current advancements. Each new development has given equipment items such as phones, tablets, and computerized cameras the ability to record, store, and sell records more easily. The expanding number of accessible motion pictures has likewise increased the desire to see them. Since then, there has been an explosion in the number of movie pictures that have attempted to explain the phenomenon. Activity centers are most useful in the areas of clinical care, athletic training, and security.

It was pleasant to see movement features everywhere. Components from all across the world are counted based on the character's movement limitations. This is done by using historical deduction or human following. As a result of these operations, the world is represented using 2D outlines [1–2]. Hu-minute Radon trans-structure descriptors are also employed at this point in time to denote a workout session. Space-time volumes can also be referred to as global features. Overlaying outlines on top of one another can be used to create spatial-worldly amounts [3, 4]. Optical stream can also be used to depict activity reality. History deduction is unnecessary. When it comes to global trademark extraction [5, 6], an optical stream-based method that tracks the movement of pixels is also used. Due to the fact that the activity descriptor can be devalued as a result of disturbance that respected in a forcefully changing foundation, this method is incredibly difficult to clamor. This is due to the fact that world focus depiction relies on explicit restriction and documented previous deduction, making it difficult from a point of view and personal appearance perspective. And it can't keep track of your activities, which makes it inferior to similar hobbies like walking and running.

In recent years, it has become more common to show local work. Also, context and character appearance are invariant. It doesn't require a precise breaking point or history derivation. On the sack-of-words mannequin [7-9], spatial-temporal characteristics are based. There are a number of basic descriptors [10-13], such as Hoard/HOF, HOG3, SURF, and MoSIFT. This portrayal has a significant flaw: they are unable to flexibly essential/shape data. Because of this, it can be used to describe a wide range of activities. There's also been an explosion of interest in human movement centers in the last few years in a worldview based on deep acing techniques. It's a far cry from the precisely crafted forms that were referenced over the course of the deep learning. When it comes to profound acing tactics, it all comes down to how the system is set up. As a result, these methods require a lot of data and a lot of limits. To solve this problem, analysts have to use sophisticated methods of analysis.

Human movement recognition was greatly enhanced by the use of outline investigation-based methodologies. [17-21] They are used to identify every global and local component. It is used in [18] and [19] to delete the global and nearby components from the movement video. For global highlights, posture correlograms and extended development records photographs are used, as mentioned by [19] The movement video in [20] is described using a three-dimensional Histogram of the configured slope [23]. The approach proposed an additional capacity that was mostly based on the poor region, which is related to the region of the individuals' embracing.

The human body is able to accurately reflect a movement. Outline key poses are no longer visible when using multi-view views in [22]. They used spatiotemporal highlights to illustrate the changes. To depict the world's capability for movement, [23] uses a binarized outline to locate the indicator fundamentally change. In [24], the shakers video mannequin the movement of an outline. There is a multi-scale volumetric approach used in [25, 26]. [26] illustrates the movement through the use of insufficient coding of photo compositions. Assessments that use outlines can also be found in more advanced learning-based systems [27, 28, and 29]. [27] combines CNN and HMM to portray long-movement video. [28] used a neurological instrument to describe the movements. This information is derived from two cortical regions - the significant cortex and the middle cortex. [29] provided a new descriptor that is fruitful of retaining the whole development data.

Fig. 1. Workflow diagram of the proposed method

Inspiration: This paper presents another trademark descriptor dependent on Finite Element Analysis (FEA) [30-31]. FEA has been utilized as a viable strategy for the auxiliary assessment of the framework. In the FEA method, the shape is changed into a limited wide assortment of components. Any place any disfigurement occurs in a body/structure these limited factors also get uprooted from their previous job and the solidness lattice of these components demonstrates how firm the body/structure is contrary to this distortion. This offers right and explicit insights about the auxiliary disfigurement of the body. Correspondingly, when a man or lady plays out an activity, his physical make-up gets disfigured in explicit examples. This propels us to follow the thought of FEA on the outlines extricated from the movement video. The proposed approach gives another close by perspectives descriptor that is completely effective of speaking to structure as pleasantly as development components of the outline.

I. Methodology of proposed framework

In Fig. 1, we can see the proposed system. The human form has been removed from the boundaries of the movement video's frame by frame. At that time, we broke down the human constitution into a series of discrete factors (triangle faces). It's at this phase that FEA is used to establish how solid the contour is. A trademark vector is used to describe solidness grids. Use of RBF-SVM classifier for activity planning.

2.1 Silhouette extraction

For example, in the proposed technique, attributes are gathered in order to distinguish specific human advances, which make the final output more significant legitimate While performing an activity, these features show the disfigurement that occurs in the outline in expressions of structure and development records of the activity. As the outline moves, so do the limited factors. The sturdy foundation of the outline highlights these points. The first step of the suggested approach is outline extraction, which is a particularly difficult problem because it needs legacy deduction. Confusion in the foundations and changes in Enlightenment thought are some of the obstacles to history deduction. While the GMM [32] has several weaknesses, it is a powerful tool for managing the basic difficulty, like a shadow. To keep track of historical deductions, we used the GMM software. As a result, the outline is removed and standardized in order to ensure uniformity in measurement across all outlines [18]. Fig. 2 recommends the video's extricated outline as a starting point for your own.

2.2 Discretization and shape work portrayal

In FEA, the first step is to discretize the problem. Figuring out how many small components make up the outline shape (see Fig. 3). (a). If you're interested in learning more about the material science of geometry, you may want to look at computer programs such as Matlab or COMSOL (for example). Our limiting component was a simple triangle object. It was a good choice. As a result of the triangle structure's use, it is believed that it is the easiest shape to represent numerical data in. A FEA toolkit included in Matlab was used for the proposed technique. Laptev et al. [10] were consulted to determine the distinct elements near the silhouette's edge. In the FEA toolkit, these factors are referred to as nodes. There are finite triangular factors used to discretize the silhouette. Since they no longer overlap, the silhouettes have been 'discreted' (distributed).

There are finite elements of triangles in Fig. 3(a). The discretized structural representation of the silhouette can be seen in Fig. 3(a), where the X-axis and Y-axis are the spatial coordinates of the triangle's vertices For examination, it offers a specific and unique picture of the total area by dividing it into smaller portions. Triangular factors are composed of three nodes each For example, each node has its own displacement in both directions, as can be seen from Figure 3. (b).

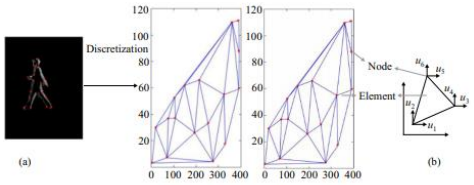

Fig. 3. (a) – Segmented discretized silhouette, (b) – displacement of a mesh (triangle) of the human body and its mesh element, (c) – deformed triangle as node 1 is displaced, (d) – triangle divided into 3 parts.

Displacement vectors of the triangle can be represented as where, U is a displacement vector for every triangular factor and u1 and u2 are the displacement of node 1 in X and Y route respectively, u3 and u4 are the displacements of node two in X and Y route and in a similar fashion u5 and u6 are the displacements of node three When silhouette strikes from one body to every other frame, nodes of the triangles are additionally displaced. To construct the face correspondence between the frames we calculated the Euclidean distance amongst the nodes of the preceding body and subsequent frame. The minimal distance will correspond to the equal points. The displacement of the nodes of the triangle is observed out from one body to some other frame. Shape characteristic [30,31] of the triangle is used to characterize the nodal displacement. Fig. 3(c) indicates the displacement of node 1 as a dotted line from its preceding factor to the displaced point, which outcomes in the deformation of the triangle if the different two nodes are fixed. Similarly, node two and node three are considered. An indoors

factor is taken internal the triangle to divide it into three areas as proven in Fig. 3(d). Let the complete region of the triangle is R and R1, R2 and R3 are the areas of three regions. This is represented via (2).

R = R1 + R2 + R3 (2)

From (2) the form features of all three areas are evaluated the use of (3)

$$J_1 = \frac{R_1}{R},\ J_2 = \frac{R_2}{R},\quad \text{and}\quad J_3 = \frac{R3}{R}, \tag{3}$$

2.3 Representation of feature vector

The displacement of the indoors factor represents the displacement of the triangle. As mentioned above the indoors factor (x, y) has displacements s in X route and t in the Y direction. Due to these displacements, a deformation is produced in the triangular element. This deformation is nothing; however the pressure developed in the triangular component in X, Y, and shear direction. These are given follows Strain in X , Y - path and shear stress are

$$\phi_x = \frac{\partial s}{\partial x} \tag{10}$$

$$\phi_y = \frac{\partial t}{\partial y} \tag{11}$$

$$\phi_x y = \frac{\partial s}{\partial y} + \frac{\partial t}{\partial x} \tag{12}$$

These strains are written in the form of matrices Once we get the strain in the triangular element of the discretized silhouette, we found out the stiffness matrix, using FEA [30-31]

$$\phi = \begin{bmatrix} \frac{\partial s}{\partial x} \\ \frac{\partial t}{\partial y} \\ \frac{\partial s}{\partial y} + \frac{\partial t}{\partial x} \end{bmatrix} \tag{13}$$

$$K_t = C^T D C t_e R_e \tag{14}$$

where, kt is the stiffness matrix for a triangle element, C is a displacement matrix situation to lines in X direction, Y direction, and shear strain, te is thickness of the physique which is steady in case of silhouette, Re is the place of the triangle and D is a consistent matrix

$$D = \frac{\xi}{1-\tau}\begin{bmatrix} 1 & \tau & 0 \\ \tau & 1 & 0 \\ 0 & 0 & \frac{1-\tau}{2} \end{bmatrix} \tag{15}$$

youngs modulus (YM) and poisson proportion (PoS) are both constant values. There are a number of parameters that have been tweaked and their attributes have been referenced in the exploratory end product space The solidity lattice of the triangle kt was converted into a one-dimensional capacity vector [19] by studying the network from apex left to posterior appropriate factor by using component analysis. The triangle's m-line and m-section firmness grid will be transformed into a one-dimensional capacity vector with m m components in its whole, as shown below. Every possible triangle in the outline was likewise assigned a vector. The full solidity framework of the shape Ks is produced by aggregating all capacity vectors of triangles. We received the following approach to help us figure out what the primary line of the Stiffness Matrix of the outline's work vector will be:

To do this, we used a discretized contour from the zenith left to the rear (inside factor of the triangle). Ks's main line will be represented by the major triangle whose inside factor is discovered first, while the triangle whose inside factor is found outstanding will characterize the rest of the column of Ks's grid. If an outline of a body is discretized into n different triangular faces, then the firmness lattice of outline Ks will have n different lines and m m quantities of the section. By using a process that is nearly equivalent to the previous one, the entire firmness framework for an outline will become the capacity vector. This capacity vector relates to the body of the movement video in a meaningful way.

Algorithm:

Given a movement video, work vectors can be created as follows.

Stage 1:
- Extraction of outlines from enter video outlines.

Stage 2:
- Extraction of recognized factors on the limit of the outlines.

Stage 3:
- Prominent elements are given as hubs to the FEA tool kit, MATLAB.

Stage 4:
- Silhouettes are discretized into limited triangular components the spot hubs go about as vertices of the triangle.

Stage 5:
- Each triangular part is spoken to by method of three hubs removal vector (U) of the triangle.

Stage 6:
- Displacement network (C) of each triangle is determined

Stage 7:
- Stiffness network (kt) is determined for each triangle with the help of removal framework C.

Stage 8:
- Complete the Stiffness network of the outlines is made by methods for joining solidness lattices (kt) of every plausible triangle of the outline.

Stage 9:
- Stiffness grid of the outline is spoken to as one-dimensional capacity vectors

Stage 10:
- Feature vector is determined for all casings of the movement video for all activities.

Stage11:
- The RBF-SVM Classifier is utilized for acknowledgment.

2.4 Dimension reduction and classification

A body of a movement video at time t is spoken to by utilizing the trademark vector extricated from the proposed technique. The size of the capacity vector of a body is

$$C = \text{row} \times \text{column}$$

of the solidness framework of the outline. Assume a movement grouping comprises of S outlines, at that point that movement arrangement has S work vectors. This impacts in an extremely unreasonable dimensional capacity space. To restrict the dimensional trademark space, we used Principal issue assessment (PCA). Further, these diminished aspects are given to RBF-SVM classifier [33-34] to catch the activities. The proposed procedure can be summed up looking like the calculation as follows

II. Experimental results

We have built up our proposed strategy on MATLAB R2015a. The proposed calculation has been inspected on a gadget having equipment setup processor Intel(R) Core (TM) i5-6200U CPU @2.30GHz 2.40 GHz with eight GB RAM and 64-piece running framework. To think about the general execution of the proposed system, precision is utilized as the general execution boundary in a forget about one cross-approval methodology.

$$TPR = \frac{TP}{TP + FN} \qquad (16)$$

$$FPR = \frac{FP}{FP + TN} \qquad (17)$$

Where, TPR speaks to invaluable cases that are effectively sorted and FRP speaks to poor occurrences that are erroneously arranged as positive. Exactness is determined as

$$Accuracy = \frac{TP + TN}{TP + TN + FP + FN} \qquad (18)$$

Specifically, Weizmann realities set [4], the KTH [35], the Ballet [36] and IXMAS[37] were selected as the datasets to be considered and evaluated by our proposed technique. There are ninety recordings in the Weizmann movement dataset. For each 2d frame, the body charge is 25 edges, and the choice is 144180 pixels. It consists of nine exceptional individuals who performed a total of ten moves, such as sprinting, bouncing, waving, bowing, and so on. Figure 4 shows an example of a body (a). Specifically, the KTH dataset contains six important actions, including applauding and waving as well as boxing. Activities at KTH were documented under four different illumination conditions, both indoors and outdoors, with one hundred accounts. A static digicam with 25 frames per second and a resolution of 160120 pixels has been used for the sum total of what accounts. Advanced camera and lighting improvements have an impact on the conditions of the KTH enlightening list accounts. In Figure 4, you can see a sample of this dataset (b).

In this expressive move dataset, a variety of on-screen characters perform highly complex smooth motion postures. Fig. 4 shows an example of a housing unit from the dataset (c). The dataset was obtained from a ballet DVD. The dataset's premise is a fundamental one. There is only one performer each video. There are forty-four recordings in the collection. This collection of recordings contains eight extraordinary and unique actions. IXMAS is a really problematic dataset where ten excellent people perform every single exercise numerous times in order to get the best results. Selected cameras were used to record these videos, which were shot from a unique perspective. As part of these actions, you might scratch your head or glance at your wristwatch. You might also stroll or sit down, for example. Because of its massive look change, intra-class assortments, self-hindrances, etc., this dataset provides unique challenges. Five outstanding computerized camera views of Xmas have been analyzed. On Fig. 4 we see an example from the IXMAS data set (d).

KTH dataset was used to fine-tune crucial boundary parameters. Almost identical settings were used to other datasets. Among these fundamental boundaries are the large variety of hubs, the reach of limited parts, and the trademark measurement using PCA's PCA-measurement system. As a result of the outline constraint, the hubs are the unique components that have been deleted. 5-10, 15-17, 20-25 notable features that have been referred to as "hubs" have been investigated. On the basis of Fig. 5.a, it's clear that when the number of recognized variables is greater than 15, we get a good result. Due to the fact that the actual precision is only 1-2 percent different whether we take various elements expanded than 17, we have taken 17 hubs in the proposed method.

In the end, the boundary is made up of several parts. It has been determined that there are a total of 10, 15, 20, 22, and 25 limited components. For example, as shown in Fig. 5(b), the number of components more than 20 is associated with greater exactness

The more discretized things we have, the more precise the delineation of the structure will be. Anyhow, the tradeoff is that more notable discretized components will increase the multifarious quality of manifestations of time. The proposed technique includes 22 amounts of triangular faces. Taking these 22 quantities of limited components, these triangles are no longer covered by the 22 quantities of limited components that are taken..

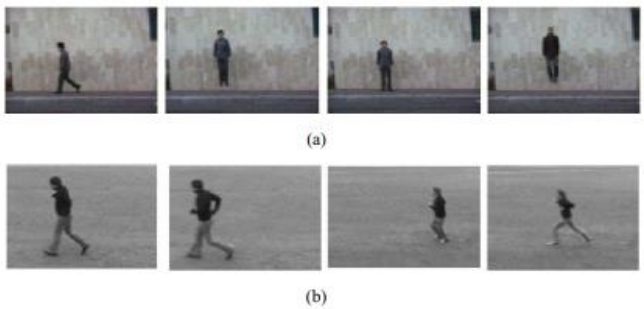

Fig. 4. Datasets:(a) Weizmann,(b) KTH,(c) Ballet,(d)– IXMAS(5 cameras)

This makes the shape simple and accomplishes higher precision. As some separation as Young's modulus alluded to in condition (15) is concerned, we have investigated its standardized qualities zero 2, zero 5, zero 7 and 1. zero as demonstrated in Fig. 5(c). We got the most ideal exactness when the expense of Young's Modulus was once zero two The attainable intention in its rear might need to be the cost of Young's modulus is more noteworthy for the rigid physical make-up and decline for the bendy body. As the human build is very bendy while playing out an activity, the decline expense zero two offers a higher outcome. The Poisson's proportion alluded to in condition (15) is utilized for the material property and it is a consistent expense that lies between 0-0. 5. In the proposed procedure we procured the streamlined final product

when the cost of used to be zero 5. The thickness of the outline referenced in condition (14) remains ordinary for all casings in a video and in the proposed system; we have accepted the expense of thickness as 1. A definitive boundary is the trademark measurement through PCA. The final product of PCA for particular measurements is spoken to in Fig. 5(d). We have investigated remarkable estimations of measurement, for example, 85, 100, 115, 130, a hundred forty five and one hundred sixty Here measurement one hundred thirty is showing higher impacts in expressions of precision and intricacy. We used the forget about one methodology for cross-approval. Tab. 1, Tab. 2, Tab. three and Tab. four recommends the disarray lattices came about because of utilizing the proposed method on the datasets Weizmann, KTH, Ballet, and IXMAS separately.

Table 1. Confusion matrix for Weizmann Dataset (R-Running, W-Walking, J-Jumping, JJ-Jumping Jack, S-Skipping, JP-Jumping at a place, SJ-Side Jumping, B-Bending, W-Waving with one hand, WB-Waving with both hands)

	R	W	J	JJ	S	JP	SJ	B	W	WB
R	0.95	0.05	0	0	0	0	0	0	0	0
W	0	1	0	0	0	0	0	0	0	0
J	0	0	1	0	0	0	0	0	0	0
JJ	0	0	0	1	0	0	0	0	0	0
S	0	0	0	0	0.96	0.04	0	0	0	0
JP	0	0	0	0	0.02	0.98	0	0	0	0
SJ	0	0	0	0	0	0	1	0	0	0
B	0	0	0	0	0	0	0	1	0	0
W	0	0	0	0	0	0	0	0	1	0
WB	0	0	0	0	0	0	0	0	0	1

Table 2. Confusion matrix for KTH Dataset (A- Applauding, WWaving, B- Boxing, WK- Walking, J-Jogging, R-Running)

	A_1	A_2	A_3	A_4	A_5	A_6
A	1	0	0	0	0	0
W	0	1	0	0	0	0
B	0	0.02	0.98	0	0	0
WK	0	0	0	1	0	0
J	0	0	0	0	0.96	0.04
R	0	0	0	0	0.02	0.98

Table 3. Confusion matrix for Ballet LR- Left to right-Hand Opening, RL- Right to left-Hand Opening, J-Jumping, H-Hopping, Swinging leg, ST-Standing, T-Turning

	A_1	A_2	A_3	A_4	A_5	A_6	A_7
LR	1	0	0	0	0	0	0
RL	0	1	0	0	0	0	0
J	0	0	0.97	0.03	0	0	0
H	0	0	0.10	0.91	0	0	0
S	0	0	0	0	1	0	0
ST	0	0	0	0	0	1	0
T	0	0	0	0	0	0	1

Table 4. Confusion matrix for IXMAS Dataset: W- Walking, WA-Waving, P- Punching, K- Kicking, T- Throwing, P- Pointing, PUPicking
Up, G- Getting Up, S- Sitting Down, TA-Turning Around, F-Folding arms, C-Checking Watch, SH-Scratching Head

	W	WA	P	K	T	P	PU	G	S	TA	F	C	SH
W	1	0	0	0	0	0	0	0	0	0	0	0	0
WA	0	0.92	0.08	0	0	0	0	0	0	0	0	0	0
P	0	0	0.97	0	0.03	0	0	0	0	0	0	0	0
K	0	0	0	1	0	0	0	0	0	0	0	0	0
T	0	0	0.03	0	0.94	0.03	0	0	0	0	0	0	0
P	0	0	0	0	0.03	0.97	0	0	0	0	0	0	0
PU	0	0	0	0	0	0	0.94	0.06	0	0	0	0	0
G	0	0	0	0	0	0	0.8	0.92	0	0	0	0	0
S	0	0	0	0	0	0	0	0	1	0	0	0	0
TA	0	0	0	0	0	0	0	0	0	1	0	0	0
F	0	0	0	0	0	0	0	0	0	0	0.97	0.03	0
C	0	0	0	0	0	0	0	0	0	0	0.04	0.94	0
SH	0	0	0	0	0	0	0	0	0	0	0	0	1

These disarray frameworks show that the greater part of the developments are a hundred percent classified excepting some tantamount sorts of activities. Subsequently, we got a precision of ninety seven 8%, ninety six 4%, ninety five 2% and ninety 3% for the Weizmann, KTH, Ballet, and IXMAS separately. We interestingly the proposed strategy with the diverse Silhouette assessment essentially based human movement discernment strategies, for example, Human Body Pose Model (HBPM) [17, 18, 22] and Human Body Pose Temporal Model (HBPTM) [19, 38] for these datasets. Chaaraoui et al. [22] separated the parts of the outline as form factors and movement is found from the multi-perspectives on cameras. The multi-see examining makes the procedure effective of separating exceptional people playing out the indistinguishable activity. Wu et al . [19] proposed the Human Body Pose Temporal Model the spot a 2-D outline veils is changed into a 1-D trademark vector. They spoke to the movement as the correlogram of stances separated from the outline. H. Han et al . [25] Represented the human constitution shapes with inadequate geometrical angles the utilization of the Bandlets change. They utilized the AdaBoost to pick the highlights. As the proposed approach offers the exceptional trade in the human build structure because of the substitute in the little factors of the outline, it makes it higher as rather than various techniques. Figure 6 display that the proposed strategy recommends a better quality outcome as opposed to various outline investigation based strategies the utilization of Weizmann, KTH, Ballet, and IXMAS datasets.

We also interestingly extraordinary most recent techniques with the proposed approach on every one of the 4 datasets in Tab. 5-Tab. eight Different evaluating procedures are utilized in these philosophies. We alluded to these evaluating procedures in Tab. s close by with the classifier that they have utilized. Tab. 5 recommends a differentiation of the proposed procedure with various systems on the Weizmann dataset. Goudelis et al. [23] proposed another trademark extraction approach dependent on the Trace Transform. They spoke to the spatiotemporal trademark in expressions of the clue fundamentally change from the binarized outline. They utilized the SVM classifier and forget about one-individual cross-approval looking at technique. They performed 94.6% precision.

The procedures [19] and [28] executed a more prominent exactness of ninety six 3% and ninety seven 3% individually. Liu et al. [28] Modeled human movement with the neural system. They utilized new capacity vectors the utilization of two cortical

regions one is the significant cortex and the second is the inside worldly cortex for movement. Afterward, they utilized the SVM classifier to comprehend the activity. The proposed strategy finished a precision of ninety seven 8%. Since we have discretized the outline into a littler triangle, practically identical developments, for example, walking and running are conspicuous higher than the various techniques.

Not at all like the Weizmann dataset, the KTH dataset presents more noteworthy troublesome conditions. It has unique arrangements having uncommon lighting installations essentials for phenomenal activities. Besides, the shadow is also an enormous task in this dataset. In this way, to manage these issues, GMM is a higher methodology for history deduction and outline extraction. Rahman et al. [38] utilized the awful space-based quality of human posture and development perspectives to mannequin the activities. To order the activities, they utilized Nearest Neighbor Classifier. The forget about one strategy is utilized for cross-approval. They affirmed a precision of

Table 5. Comparison of the proposed method with similar methods on Weizmann dataset

Method	Year	Classifier and Test Scheme	Accuracy
[25]	2015	SVM	81.5
[22]	2013	KNN, LOSO	91.7
[19]	2013	SVM, LOSO	96.3
[23]	2013	SVM, LOPO	94.6
[24]	2014	KNN, LOO	91.4
[26]	2017	NNC	95.3
[27]	2016	CNN-HMM	90.1
[28]	2017	SVM	97.3
Proposed Method		SVM, LOO	97.8

Table 6. Comparison of the proposed method with similar methods on KTH dataset

Method	Year	Classifier and Test Scheme	Accuracy
[25]	2015	Adaboost, SVM, LOO	94.2
[23]	2013	SVM, LOPO	92.7
[26]	2017	NNC, LOO	93.6
[27]	2016	CNN-HMM	94.4
[28]	2017	SVM	91.3
[38]	2014	KNN, LOO	95.1
[39]	2015	KNN	90.8
[29]	2017	CNN-RNN	95.8
Proposed Method		SVM, LOO	96.4

Table 7. Comparison of the proposed method with similar methods on Ballet dataset

Method	Year	Classifier and Test Scheme	Accuracy
[17]	2017	SVM-NN, LOOCV	94.2
[18]	2015	SVM-NN, LOOCV	93.8
[41]	2009	S-CTM, LOO	89.8
[42]	2014	RVM, LOO	90.4
[43]	2014	SVM, LOO	90.3
Proposed Method		SVM, LOOCV	95.2

Table 8. Comparison of the proposed method with similar methods on IXMAS dataset

Method	Year	C1	C2	C3	C4	C5	Overall Accuracy
[44]	2011	89.1	83.4	89.3	87.2	89.2	87.8
[45]	2010	84.2	85.2	84.1	81.5	82.6	82.7
[46]	2013	86.5	83.8	86.1	84.5	87.4	87.2
[47]	2016	91.3	85.7	89.3	90.2	86.5	87.5
Proposed Method		90.8	90 .6	92.4	91.2	90.6	90.2

95. 1% as demonstrated in Tab. 6. In each other strategy, Shi et al. [29] proposed new development descriptor consecutive profound direction descriptors for extensive timeframe development video. The CNN-RNN people group is utilized to investigate the movement. They finished a same precision of ninety five 8% as opposed to [38]. We have utilized a forget about one methodology and the proposed approach executed ninety six 4% precision which is higher than various strategies.

Table 7 recommends an appraisal of the proposed approach with the diverse condition of-the-techniques for the Ballet dataset. Vishwakarma et al. [18] utilized outline based assessment and separated the trademark vectors dependent on human stances. They have utilized SVM, LDA and Neural Network-based crossover classifiers to comprehend the activity. They achieved a precision of ninety three 8%. Vishwakarma et al. [17] utilized another outline assessment the spot they originally situated out the normal force image of an outline. The spatial dispersion of angle is used on regular force picture to make it a global capacity and the fleeting capacity is resolved out with the guide of Radon fundamentally change of the outlines. These focuses are given to the crossover classifier and they increase a more prominent precision of ninety four 2%. In every method [17] and [18] they utilized forget about one cross-approval. The proposed approach recommends higher precision of ninety five 3%. As referenced above discretized outline into little triangles help to comprehend the moves in an expressive dataset like Ballet move. In this dataset, the cautiously the entertainer's appearances are found the higher impacts might need to be accomplished.

Contractions utilized in Tab. 5-Tab. eight are SVM: help vector machine, KNN: k-closest neighbor, LOSO: forget about one-arrangement -, LOPO: forget about one-individual, LOO: forget about one, NNC: closest neighbor classifier, CNN: convolution neural system, HMM: concealed Markov model, RNN: repetitive neural system, SVM-NN: help vector machine-neural system, LOOCV: forget about one cross-approval, S-CTM, RVM: significance vector machine. IXMAS dataset has 5 stand-out advanced camera sees. Techniques [42, 46-47] show about similar correctnesses which are round 87%. Wang et al . [47] utilized the Bag-of-visual word strategy dependent on neighborhood highlights. At that point they utilized the cross-see technique to manage the issue of view exchange because of particular cameras. The proposed approach has performed more prominent Accuracy for all the perspectives. We purchased a normal of ninety 2%

precision. To manage the difficulty of variation in viewpoint we utilized view-invariant diversion factor on the limit of the outline which went about as the vertices of the triangles for the term of the discretization step. Tab. eight recommends an evaluation of the proposed approach the diverse condition of-the-strategies for IXMAS dataset for run-time investigation, we have utilized NVIDIA GPU and MATLAB 2015a with a Parallel processing tool kit. Time taken for different modules in the proposed approach is determined. We have broke down the run-time of the proposed approach on all the datasets referenced previously. The basic run-time of the proposed dataset and is given underneath stepwise:

Extraction of silhouette from motion video (Sec): 0.41
Silhouette discretization into triangular faces (Sec): 0.54
Calculation of the silhouette stiffness matrix (Sec): 1.45
Classification (Sec): 0.52
Total time for motion awareness (Sec): 2.92

Thus, the run-time of the proposed technique is pretty good.

III. CONCLUSION

Finite Element Analysis is another way to understand human development (FEA). Applying a second descriptor for recognizing the video diagrams' boundaries, which is based on the strength system's isolated edges, is a good idea. In addition, this approach is able to eliminate each shape as well as motion information. The RBF-SVM classifier receives the trademark vectors that were deleted from the suggested technique. Approval of the suggested strategy was completed in a highly irritating manner. The framework's biggest problem is that it requires accurate diagram extraction. However, the proposed technique implies that it is superior to other current strategies of applying them on challenging general datasets, such as the Weizmann, KTH, Ballet and IXMAS datasets, among others.

References

[1] A. F. Bobick and J. W. Davis, "The recognition of human movement using temporal templates," IEEE Trans. Pattern Anal. Machine Intell., vol. 23, no. 3, pp. 257-267, 2001 [doi:10.1109/34.910878].

[2] R. Souvenir and J. Babbs, "Learning the viewpoint manifold for action recognition, IEEE International Conference on Computer Vision Pattern Recognition (CVPR'08),", 2008, pp. 1-7.

[3] M. Blank et al., Action as Space–Time Shapes, IEEE International Conference on Computer Vision (ICCV'05), vol. 2, 2005, pp. 1395-1402.

[4] L. Gorelick et al., "Action as space–time shapes," IEEE Trans. Pattern Anal. Mach. Intell., vol. 29, no. 12, pp. 2247-2253, 2007 [doi:10.1109/TPAMI.2007.70711].

[5] K. Guo et al., "Action recognition from video using feature covariance matrices," IEEE Trans. Image Process., vol. 22, no. 6, pp. 2479-2494, 2013 [doi:10.1109/TIP.2013.2252622].

[6] Y. Chen et al., "A spatio-temporal interest point detector based on vorticity for action recognition, IEEE International Conference on Multimedia Expo Workshop,", 2013, pp. 1-6.

[7] M. Laptev et al., "Learning realistic human actions from movies, IEEE Conference on Computer Vision Pattern Recognition,", 2008, pp. 1-8.

[8] S. Savarese et al., "Spatial-temporal correlations for unsupervised action classification,", Proc. of the IEEE Workshop on Motion Video Computing, 2008, pp. 1-8.

[9] S. Ryoo and J. K. Aggarwal, "Spatio-temporal relationship match: Video structure comparison for recognition of complex human activities, IEEE." 12th Intl. Conf. on Comput. Vis., 2009, pp. 1593-1600.

[10] I. Laptev and T. Lindeberg, "Space–time interest points,", Proc. Ninth IEEE Intl. Conf. on Computer Vision, 2003, pp. 432-439.

[11] A. Klaser et al., "A spatio-temporal descriptor based on 3D-gradients,", Proc. British Machine Vision Conf., 2008, pp. 995-1004.

[12] G. Willems et al., "An efficient dense scale-invariant spatio-temporal interest point detector, ECCV," vol. 5303, pp. 650-663, 2008.

[13] M. Chen and A. Hauptmann, MoSIFT: Recognizing Human Actions in Surveillance Videos, CMU-CS-09-161 2009.

[14] N. Ballas et al., "Delving deeper into convolutional networks for learning video representations, International Conference on Learning Representations 2016.".

[15] L. Wang et al., "Action recognition with trajectory pooled deep-convolutional descriptors, IEEE Conference on Computer Vision Pattern Recognition,", 2015, pp. 4305-4314.

[16] L. Sun et al., "Human action recognition using factorized spatio-temporal convolutional networks, IEEE International Conference on Computer Vision (ICCV),", 2015, pp. 4597-4605.

[17] D. K. Vishwakarma and K. Singh, "Human activity recognition based on the spatial distribution of gradients at sub-levels of average energy silhouette images, IEEE," Trans. Cogn. Dev. Syst., vol. 9, no. 4, pp. 316-327, 2017.

[18] D. K. Vishwakarma and R. Kapoor, "Hybrid classifier based human activity recognition using the silhouettes ands cells," Expert Syst. Appl., vol. 42, no. 20, pp. 6957-6965, 2015 [doi:10.1016/j.eswa.2015.04.039].

[19] D. Wu and L. Shao, "Silhouette analysis-based action recognition via exploiting human poses," IEEE Trans. Circuits Syst. Video Technol., vol. 23, no. 2, pp. 236-243, 2013 [doi:10.1109/TCSVT.2012.2203731].

[20] D. Weinland et al., "Making action recognition robust to occlusions viewpoint changes,", Lecture Notes in Computer Science European Conf. on Comput. Vis. (ECCV), pp. 635-648, 2010 [doi:10.1007/978-3-642-15558-1_46].

[21] B. Saghafi and D. Rajan, "Human action recognition using Pose-based discriminant embedding," Signal Process. Image Commun., vol. 27, no. 1, pp. 96-111, 2012 [doi:10.1016/j.image.2011.05.002].

[22] A. A. Chaaraoui et al., "Silhouette-based human action recognition using sequences of key poses," Pattern Recognit. Lett., vol. 34, no. 15, pp. 1799-1807, 2013 [doi:10.1016/j.patrec.2013.01.021].

[23] G. Goudelis et al., "Exploring trace transform for robust human action recognition," Pattern Recognit., vol. 46, no. 12, pp. 3238-3248, 2013 [doi:10.1016/j.patcog.2013.06.006].

[24] R. Touati and M. Mignotte, "MDS-based multi-axial dimensionality reduction model for human action recognition, Canadian Conference on Computer Robot Vision,", 2014, pp. 262-267.

[25] H. Han and X. J. Li, "Human action recognition with sparse geometric features," Imaging Sci. J., vol. 63, no. 1, pp. 45-53, 2015 [doi:10.1179/1743131X14Y.0000000091].

[26] Y. Fu et al., "Sparse coding-based space–time video representation for action recognition," Multimedia Tool. Appl., vol. 76, no. 10, pp. 12645-12658, 2017 [doi:10.1007/s11042-016-3630-9].

[27] J. Lei et al., "Continuous action segmentation recognition using hybrid convolutional neural network-hidden Markov model," IET Comput. Vis., vol. 10, no. 6, pp. 537-544, 2016.

[28] H. Liu et al., "Computational model based on the neural network of visual cortex for human action recognition," IEEE Trans. Neural Netw. Learn. Syst., vol. 29, no. 5, pp. 1427-1440, 2017.

[29] Y. Shi et al., "Sequential deep trajectory descriptor for action recognition with threestream CNN," IEEE Trans. Multimedia, vol. 19, no. 7, pp. 1510-1520, 2017 [doi:10.1109/TMM.2017.2666540].

[30] "2D triangular elements, the University of New Mexico", http: //www.unm, edu/bgreen/ME360/2D%20Triangular %20 Elements.pdf.

[31] D. K. Jha et al., "An accurate two dimensional theory for deformation stress analysis of functionally graded thick plates," Int. J. Adv. Struct. Eng., pp. 6-7, 2014.

[32] J. Dou and J. Li, "Robust human action recognition based on spatiotemporal descriptors motion temporal templates," Optik, vol. 125, no. 7, pp. 1891-1896, 2014 [doi:10.1016/j.ijleo.2013.10.022].

[33] Q. Song et al., Robust Support Vector Machine for Bullet Hole Image Classification, IEEE Transaction on Systems Man Cybernetics, vol. 32no., pp. 440-448, 2002.

[34] S. S. Keerthi and C. J. Lin, "Asymptotic behaviors of support vector machines with Gaussian kernel," Neural Comput., vol. 15, no. 7, pp. 1667-1689, 2003 [doi:10.1162/089976603321891855].

[35] C. Schuldt et al., "R, ognizing human actions: A local SVM approach,", Proc. 17th Intl. Conf. on Pattern Recognition Cambridge, UK, 2004.

[36] T. Guha and R. K. Ward, "Learning sparse representations for human action recognition," IEEE Trans. Pattern Anal. Mach. Intell., vol. 34, no. 8, pp. 1576-1588, 2012 [doi:10.1109/TPAMI.2011.253].

[37] D. Weinland et al., "Free viewpoint action recognition using motion history volumes," Comput. Vis. Image Underst., vol. 104, no. 2-3, pp. 249-257, 2006 [doi:10.1016/j.cviu.2006.07.013].

[38] S. A. Rahman et al., "Fast action recognition using negative space features," Expert Syst. Appl., vol. 41, no. 2, pp. 574-587, 2014 [doi:10.1016/j.eswa.2013.07.082].

[39] I. Gómez-Conde and D. N. Olivieri, "A KPCA spatio-temporal differential geometric trajectory cloud classifier for recognizing human actions in a CBVR system," Expert Syst. Appl., vol. 42, no. 13, pp. 5472-5490, 2015 [doi:10.1016/j.eswa.2015.03.010].

[40] L. Juan and O. Gwun, "A comparison of SIFT, PCA-SIFT and SURF," Int. J. Image Process., vol. 3, no. 4, pp. 143-152, 2009.

[41] Y. Wang and G. Mori, "Human action recognition using semilatent topic models," IEEE Trans. Pattern Anal. Mach. Intell., vol. 31, no. 10, pp. 1762-1774, 2009 [doi:10.1109/TPAMI.2009.43].

[42] L.-M. Xia et al., "Human action recognition based on chaotic invariants," J. Cent. South Univ. University,, vol. 20, no. 11, pp. 3171-3179, 2013 [doi:10.1007/s11771-013-1841-z].

[43] A. Iosifidis et al., "Discriminant bag of words based representation for human action recognition," Pattern Recognit. Lett., vol. 49, no. 1, pp. 185-192, 2014 [doi:10.1016/j.patrec.2014.07.011].

[44] X. Wu et al., "Action recognition using context appearance distribution features, IEEE Conference on Computer Vision Pattern Recognition (CVPR),", 2011, pp. 489-496.

[45] [D, M. Weinland et al., "Making action recognition 'robust to occlusions viewpoint changes', European Conference on Computer Vision (ECCV),", 2010, pp. 635-648.

[46] E. A. Mosabbeb et al., "Multi-view human activity recognition in distributed camera sensor networks" Sensors, vol. 13, no. 7, pp. 8750-8770, 2013 [doi:10.3390/s130708750].

[47] J. Wang et al., "Cross-view action recognition based on a statistical translation framework," IEEE Trans. Circuits Syst. Video Technol., vol. 26, no. 8, pp. 1461-1475, 2016 [doi:10.1109/TCSVT.2014.2382984].